



OPEN

DATA DESCRIPTOR

A dataset to assess mobility changes in Chile following local quarantines

Luca Pappalardo¹, Giuliano Cornacchia^{1,2}, Victor Navarro³, Loreto Bravo^{3,4}
& Leo Ferres^{3,4,5}✉

Fighting the COVID-19 pandemic, most countries have implemented non-pharmaceutical interventions like wearing masks, physical distancing, lockdown, and travel restrictions. Because of their economic and logistical effects, tracking mobility changes during quarantines is crucial in assessing their efficacy and predicting the virus spread. Unlike many other heavily affected countries, Chile implemented quarantines at a more localized level, shutting down small administrative zones, rather than the whole country or large regions. Given the non-obvious effects of these localized quarantines, tracking mobility becomes even more critical in Chile. To assess the impact on human mobility of the localized quarantines, we analyze a mobile phone dataset made available by Telefónica Chile, which comprises 31 billion eXtended Detail Records and 5.4 million users covering the period February 26th to September 20th, 2020. From these records, we derive three epidemiologically relevant metrics describing the mobility within and between comunas. The datasets made available may be useful to understand the effect of localized quarantines in containing the COVID-19 pandemic.

Background & Summary

As of September 2022, the COVID-19 pandemic is a global threat that resulted in around 600 million infected people and more than six million deaths globally¹. In South America, Chile is among the most severely affected countries, with more than 4.6 million infected people and a death toll that surpassed the 60,000 mark as of September 2022. Similarly to other severely affected countries^{2–9}, Chile implemented Non-Pharmaceutical Interventions (NPIs) such as regional lockdown, stay-at-home orders, and travel restrictions, in an attempt to mitigate the COVID-19 epidemics through reducing individual mobility and promoting social distancing. In contrast with countries such as China, Italy, and the USA, which implemented NPIs at the national or regional level^{2,6,8,9}, Chile's implemented NPIs at the comuna level. Comunas, also known as municipalities or communes in other countries, are the smallest administrative (political) subdivision in Chile^{10,11}. There are 346 comunas in Chile. Without counting Antártica, the largest comuna with an area of 1.25 million square kilometres, the remaining 345 comunas have a mean area of 2,199 km² (stdev. 4,824 km²), with the smallest being San Ramón, Lo Prado, Lo Espejo, and Independencia, with 7 km² each, and the largest is Natales in the Magallanes region, with an area of 4,8974 km². Two comunas in the same region may be regulated by different NPIs: whereas one is in lockdown, adjacent ones might have no travel restrictions. Only one comuna, Santiago, was split in half in terms of NPIs, with one half under quarantine while the other not. Given the peculiarity of NPIs' spatial scale in Chile, tracking mobility changes at the comuna level is crucial to assess local quarantines' efficacy and measure the effect of mobility reductions on predicting the virus spread¹². While indices of changes in human mobility do exist at the regional level in Chile (e.g., the Google Mobility Reports¹³), there are no official indices at the comuna level.

Mobile phone records provide an unprecedented opportunity in tracking human movements^{14–18}, allowing for estimating presences and population density^{19–21}, mobility patterns^{16,22–26}, flows^{27–30}, and socio-economic status^{31–36}. When used correctly and adequately aggregated to preserve privacy^{37–40}, mobile phone data represent a crucial tool for supporting public health actions across the phases of the COVID-19 pandemic^{12,41}. Motivated by the potential of mobile phone data in capturing the geographical spread of epidemics^{42–45}, researchers and

¹ISTI-CNR, Pisa, Italy. ²Department of Computer Science, University of Pisa, Pisa, Italy. ³Faculty of Engineering, Universidad del Desarrollo, Santiago, Chile. ⁴Telefónica R&D Santiago, Providencia, Chile. ⁵ISI Foundation, Turin, Italy. ✉e-mail: lferres@udd.cl

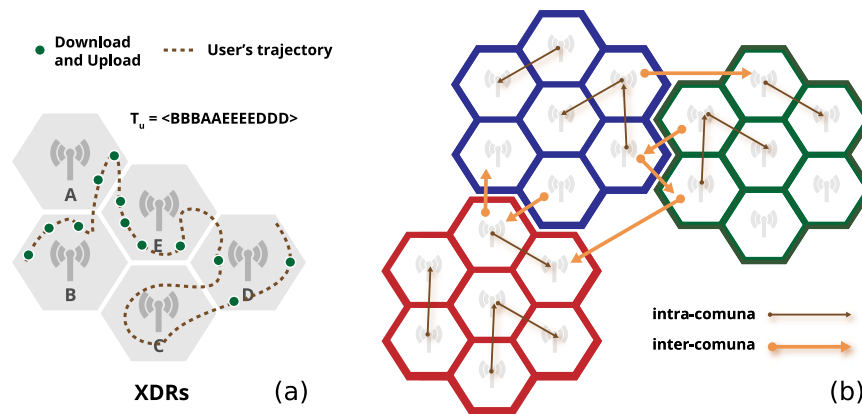


Fig. 1 (a) Illustrative example of eXtended Detail Records (XDRs) of a mobile phone user. The hexagons represent mobile phone towers and green dots the positions where the user starts a download/upload operation. The dotted line indicates the real movement of the user, from the left to the right. (b) Intra-comuna movements (black arrows) and inter-comuna movements (orange arrows). Hexagons of the same color indicate towers that fall in the same comuna.

region	rid	comuna	cid	area	IM_{int}	IM_{ext}	IM	date
Los Ríos	14	Valdivia	14101	1018.32	6.21	0.91	7.13	2020-02-26
Los Ríos	14	Valdivia	14101	1018.32	6.42	0.93	7.35	2020-02-27
Los Ríos	14	Valdivia	14101	1018.32	6.75	1.08	7.84	2020-02-28
Los Ríos	14	Valdivia	14101	1018.32	6.88	1.17	8.05	2020-02-29
Los Ríos	14	Valdivia	14101	1018.32	5.58	1.05	6.63	2020-03-01

Table 1. Structure of the released dataset.

qid	comuna	status	coverage	start	end	cid	area	perimeter
4	El Bosque	Active	whole	2020-04-16	—	13105	2.06e7	1.87e4
26	Quinta Normal	Active	whole	2020-04-23	—	13126	1.70e7	2.12e4
38	Cerrillos	Active	whole	2020-05-05	—	13102	2.41e7	2.52e4
42	Conchalí	Active	whole	2020-05-08	—	13104	1.59e7	1.68e4

Table 2. Structure of the quarantines dataset.

governments have started to collaborate with mobile network operators to estimate the effectiveness of control measures in several countries^{2,10,46–50}.

To assess the impact of the NPIs imposed by Chilean authorities in response to the epidemics, we analyse a mobile phone dataset provided by Telefónica Chile, which comprises 31 billion eXtended Detail Records (XDRs) and 5.4 million users distributed all over the country covering the period February 26th, 2020 to September 20th, 2020. An XDR is created every fifteen minutes if a certain threshold of traffic has been reached, thus describing individual movements in great detail²¹. From the XDRs, we derive three epidemiologically relevant metrics: the Index of Internal Mobility (IM_{int}), which quantifies the amount of mobility within each comuna of the country; the Index of External Mobility (IM_{ext}), quantifying the mobility between comunas; and the Index of Mobility (IM), which considers any movement, both within and between comunas. We analyse how these metrics change as the COVID-19 epidemics spread out in Chile, highlighting a considerable heterogeneity of response to local quarantines across the country.

The datasets we make available will grow as time goes by and, to the best of our knowledge, are the only ones describing mobility changes and dates of local quarantines in Chile at the comuna level. They can be used not only for fighting against the COVID-19 epidemics but will also benefit other research and applications such as emergency response^{51,52} and crowd flow prediction^{14,53–55}. The datasets described are currently used at all levels of the Chilean government.

Methods

Mobile phone operators collect several different streams of mobile phones interaction with the cellular network for billing and operational purposes. Among them are the eXtended Detail Records (XDRs), a mixture of human- and device-driven event, triggered either by explicitly requesting an HTTP address or automatically downloading content from the Internet (e.g., emails) every 15 minutes and at certain traffic thresholds.

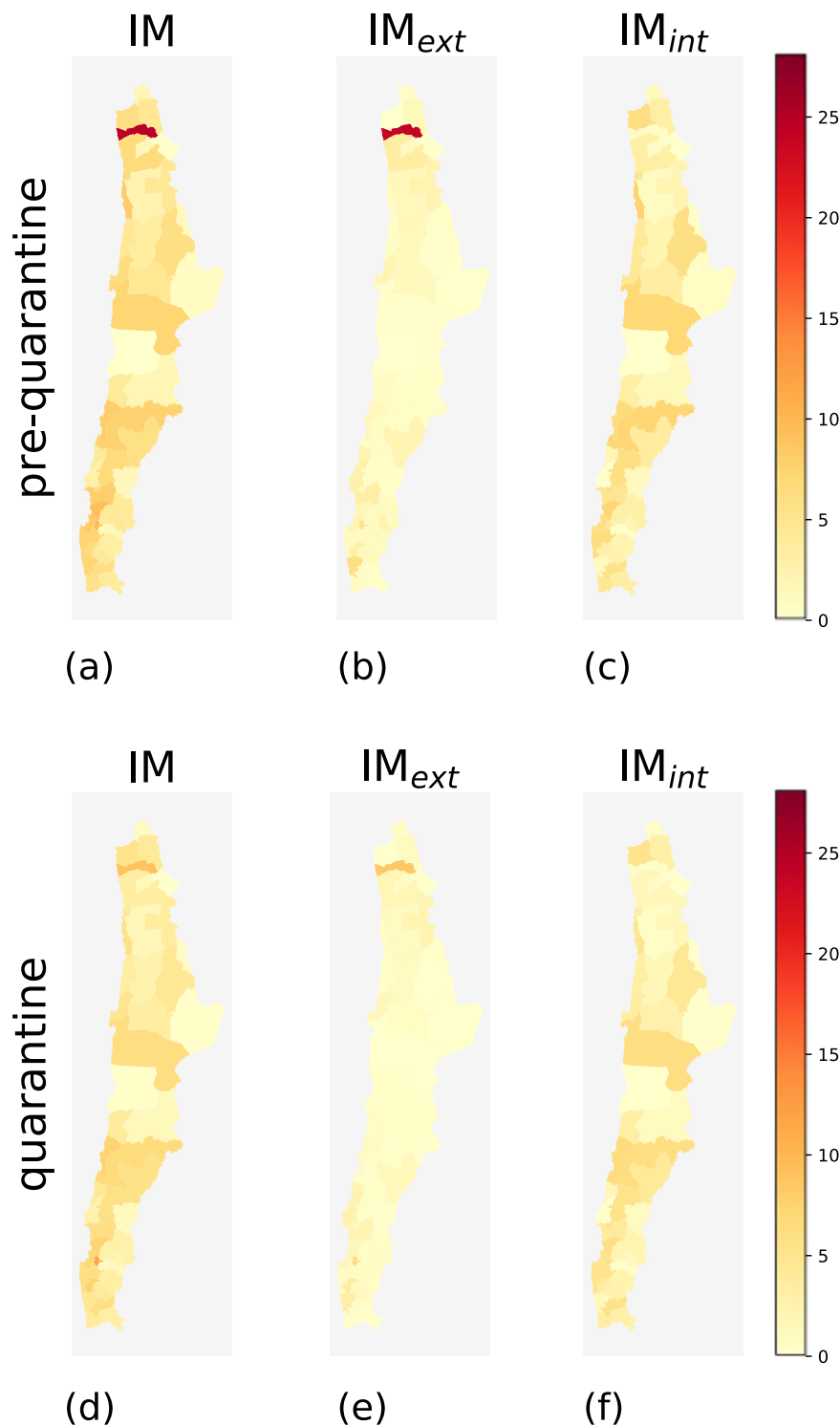


Fig. 2 Choropleth maps of IM , IM_{int} and IM_{ext} for the comunas in northern Chile for the pre-quarantine (first row) and the quarantine (second row) periods.

Formally, an XDR is a tuple (u, t, A, k) , in which there is only one tower A involved, u is the caller's identifier, t is a timestamp of when the record is created, and k is the amount of downloaded information (Fig. 1a). Rather than capturing trips, we are interested in detecting any “movement”, i.e., any transition between two antennas. From an epidemiological point of view, transitions provide a useful indication of people's displacements and hence useful information about the movements of the virus between areas within the same comuna or between two comunas. Even if an individual's movement between two antennas may not be a trip from a semantic point of view, it denotes the movement of the virus between those two antennas anyway. To this purpose, from the XDRs of the individuals, we define two types of movement. Every time a user moves from one tower to another

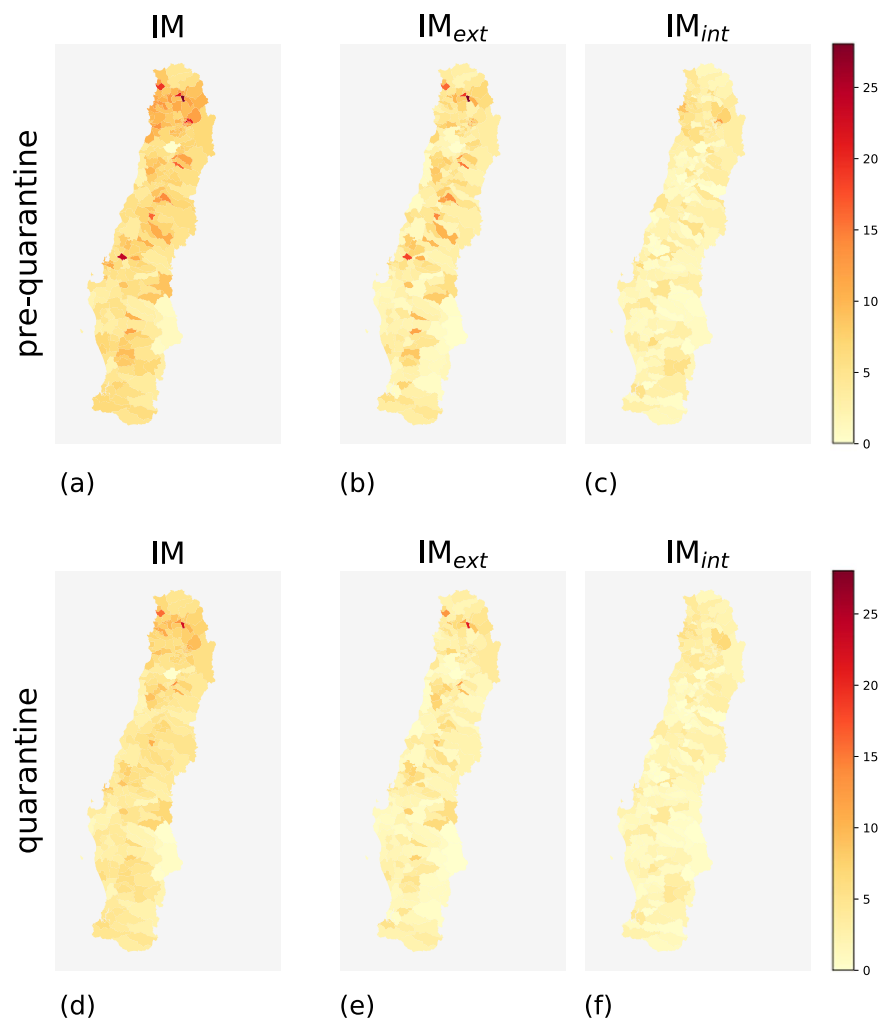


Fig. 3 Choropleth maps of IM, IM_{int} and IM_{ext} for the comunas in central Chile for the pre-quarantine (first row) and the quarantine (second row) periods.

within the same comuna, they generate an intra-comuna movement. Every time the user moves from an tower to another in a different comuna, they generate an inter-comuna movement (Fig. 1b). For each day and comuna, we construct three indicators of mobility based on the intra- and inter-comuna movements:

1. IM_{int} (Index of Internal Mobility), the number of intra-comuna movements for that day;
2. IM_{ext} (Index of External Mobility), the number of inter-comuna movements for that day;
3. $IM = IM_{int} + IM_{ext}$ (Index of Mobility).

All the three indices ranges in $[0, \infty)$, where a value of 0 indicates no mobility at all. We normalize the three indices with respect to the number of users that reside in the comuna, estimated as the total number of unique mobile devices whose home tower falls in that comuna. Each device's home tower is computed as the tower in which it has the highest number of XDRs during nighttime (between 7 pm and 7 am, inclusive)^{21,56}. The number of estimated resident users in the comunas is strongly correlated ($R^2 = 0.96$, slope = 4.37, intercept = 298.30) with the official population of the comunas as per the official 2017 Chilean Census.

Data Records

The raw datasets were provided by Telefónica/Movistar Chile, a mobile phone company which possesses between 29–32% of the Chilean mobile phone market. Telefónica gathers data for billing purposes and for network maintenance purposes by persisting network events. Users are not allowed to “opt-out” of billing information, as stated in the terms and conditions below. They are, however, able to opt out of the use of personal data by calling a number or visiting the Telefónica website (see page 3, section 6) of Telefónica's Terms and Conditions (see⁵⁷ in Spanish). In this study, no personal data or information whatsoever is used in the creation of the dataset proposed here (in fact, it's only the aggregated number of transitions between rtowe)s, without any individual information.

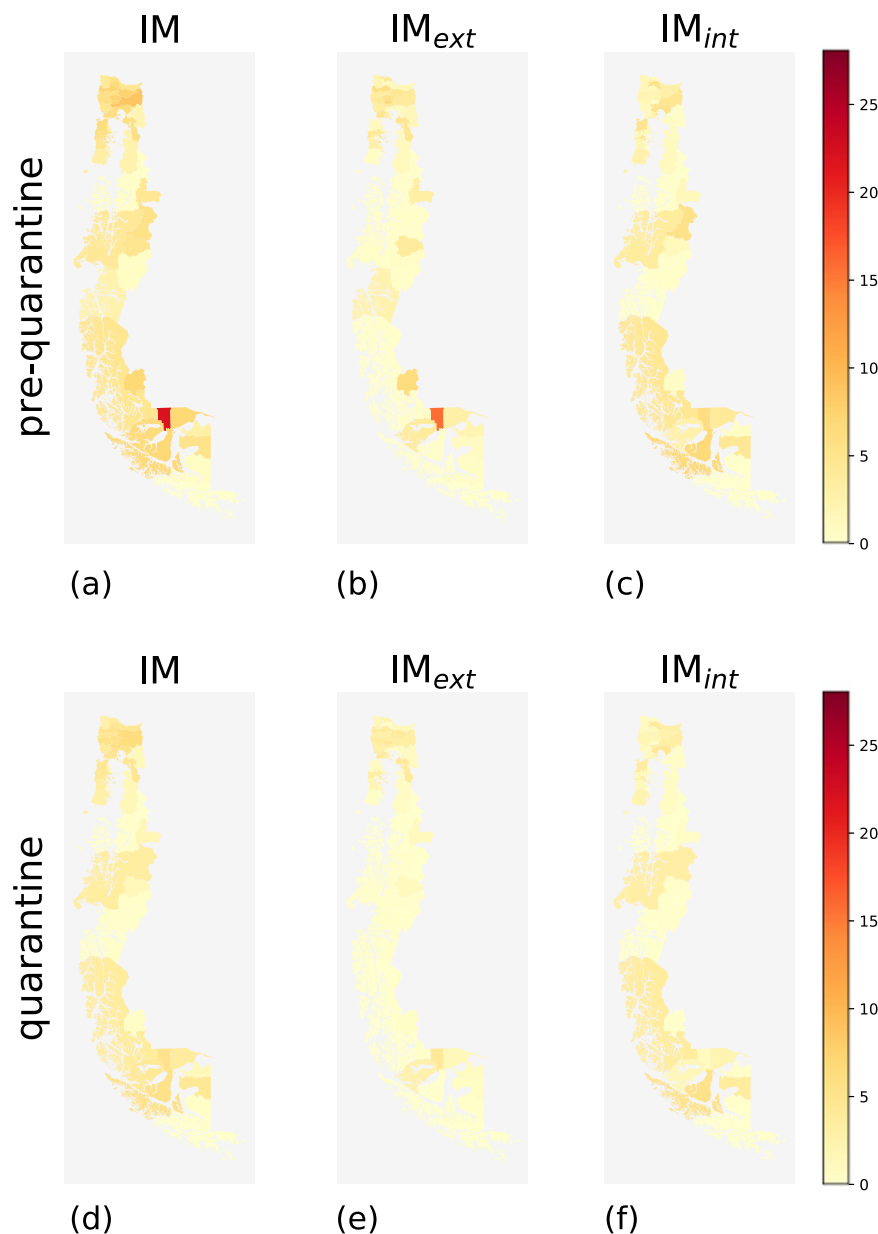


Fig. 4 Choropleth maps of IM, IM_{int} and IM_{ext} for the comunas in southern Chile for the pre-quarantine (first row) and the quarantine (second row) periods.

From the raw datasets we construct the three mobility indices described above. The datasets are released under the CC BY 4.0 License and are publicly available at⁵⁸. Table 1 shows the structure of the dataset describing the mobility indices. Each record refers to a comuna in Chile and describes:

- the official name of the region (region, type:string);
- the identifier of the region as per the official 2017 Chilean Census (rid, type:string);
- the official name of the comuna (comuna, type:string);
- the identifier of the comuna as per the official 2017 Chilean Census (cid, type:string). All maps and their official identifiers can be downloaded from the National Statistics Office of Chile⁵⁹;
- the area of the comuna in km² (area, type:float);
- the values of IM, IM_{int} and IM_{ext} for that day (type:float);
- the day the IM, IM_{int} and IM_{ext} values refer to (date, type:date).

Table 2 shows the structure of the quarantines dataset. Each record refers to a quarantine regulation and describes:

- the identifier of the quarantine regulation (qid, type:integer);
- the official name of the comuna (comuna, type:string);

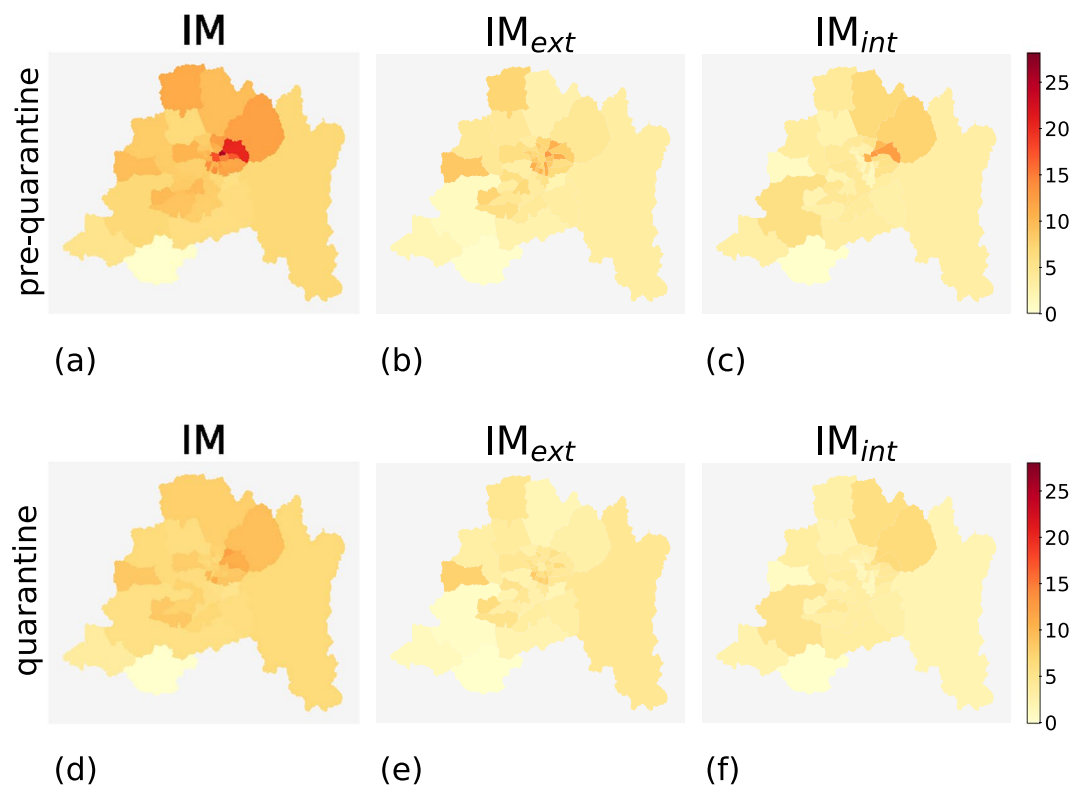


Fig. 5 Choropleth maps of IM , IM_{int} and IM_{ext} for the comunas in the metropolitan area of Santiago de Chile for the pre-quarantine (first row) and the quarantine (second row) periods.

Pre-quarantine period					
	Comuna	Region	IM	IM_{ext}	IM_{int}
1	Rinconada	Valparaíso	30.37	27.96	2.42
2	Providencia	Metropolitana de Santiago	25.29	12.58	12.71
3	Camarones	Arica y Parinacota	24.62	23.77	0.85
4	Ranquil	Ñuble	23.87	18.33	5.54
5	Laguna Blanca	Magallanes	21.92	15.75	6.18
6	Panquehue	Valparaíso	20.93	19.02	1.90
7	Vitacura	Metropolitana de Santiago	20.40	10.54	9.86
8	Las Condes	Metropolitana de Santiago	20.22	7.79	12.42
9	Zapallar	Valparaíso	19.26	15.98	3.28
10	Santiago	Metropolitana de Santiago	17.44	6.97	10.48

Table 3. Values of IM , IM_{ext} and IM_{int} of the ten comunas with the highest IM computed between March 9th and March 15th, 2020. As an example, Rinconada (Valparaíso region) has $IM = 30.37$, meaning that the number of movements within, to, or from that comuna is around 30 times higher than the estimated number of users that reside in Rinconada.

- the status of the quarantine, that can be either active or not active (status, type:string);
- the coverage of the quarantine, that can be either partial, rural, or complete (coverage, type:string);
- the date the quarantine started (start, type:date);
- the date the quarantine ended, which is “-” if it is still active (end, type:date);
- the identifier of the comuna as per the official 2017 Chilean Census (cid, type:string);
- the area of the quarantine in m^2 (area, type:float);
- the perimeter of the quarantine (perimeter, type:float).

A limitation of all phone-records studies concerns the position of towers and the geographical area they “illuminate” or serve given their technical specifications. There may be towers that serve two neighboring comunas, for example, impacting our movement counts. However, two phenomena mitigate this problem: (i) comunas are generally large, and eventual borderline events are scarce given the 15-minute span; and (ii) telco companies do not record all antenna interactions by mobile devices, because storing all that information would be costly.

Quarantine period					
	Comuna	Region	IM	IM _{ext}	IM _{int}
1	Rinconada	Valparaíso	22.44	21.09	1.35
2	Zapallar	Valparaíso	15.84	13.16	2.68
3	Panquehue	Valparaíso	13.30	11.13	2.17
4	Coinco	Libertador Gen. B. O'Higgins	13.20	12.36	0.84
5	Andacollo	Coquimbo	11.85	6.25	5.60
6	Vitacura	Metropolitana de Santiago	11.33	4.29	7.04
7	Limache	Valparaíso	11.25	5.41	5.84
8	La Reina	Metropolitana de Santiago	10.78	6.16	4.62
9	Concón	Valparaíso	10.75	4.69	6.06
10	Villa Alegre	Maule	10.67	8.67	1.99

Table 4. Values of IM, IM_{ext} and IM_{int} of the ten comunas with the highest IM computed over the period from June 22nd and June 28th, 2020. As an example, Rinconada (Valparaíso region) has IM = 22.44, meaning that the number of movements within, to, or from that comuna is around 22 times higher than the estimated number of users that reside in Rinconada.

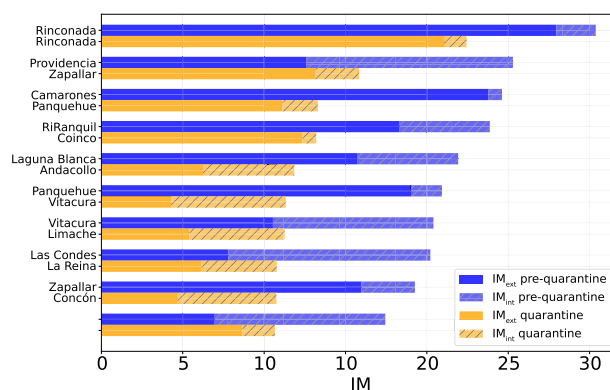


Fig. 6 Values of IM, IM_{int}, and IM_{ext} of the comunas in the top 10 ranking computed for the pre-quarantine and quarantine period. The coupled bars represent comunas corresponding to the same position in the rank.

In our case, an event (a phone record or XDR) is typically generated every y minutes and if and only if the device has crossed a threshold of x MegaBytes (MBs) of traffic (not revealed by the company as it is an industrial secret). A two-rule heuristic determines the quantities x and y . A “clock” triggers a rule every 15 minutes: if the user has reached x MBs at either 15, 30, or 45 minutes, the system appends a new XDR in the database. Some heavy users will use up the x MBs threshold at 15 minutes (if they are watching movies on the web, for instance), most at 30 minutes, and a few light users will reach the threshold at 45 minutes. There is also a fair share of frequency at other times. The second rule states that if the control plane of the mobile network notices some particular phone events, such as some antenna handovers, turning off the phone, or losing connection, then a record is created into the database at any time (irrespective of the megabytes used), making it possible to find events anywhere in-between the clock’s 15-minute triggers.

Technical Validation

In our analysis, we consider two periods: the pre-quarantine period, from March 9th to March 15th, 2020, and the quarantine period, from June 22nd to June 28th, 2020. Although we have two weeks before March 9th, the transition from February to March marks the start of the Fall school semester in Chile. In 2020, March 6th was the start of the semester, so we assume that the “business as usual” period would be best represented by the week of March 9th until March 15th. March 16th marked the start of NPIs in Chile, with the closure of schools, universities and large public gatherings. After that, on March 26th, there was a partial lockdown of seven comunas in the Metropolitan Region. By June 22–28, more than half of the population of the country was under quarantine, and mobility was at 40% reduction.

During the pre-quarantine period, comunas with high mobility indices and comunas with low mobility indices coexist. Geographically, high-mobility comunas are concentrated near urban areas such as the capital Santiago and, in general, in the center of the country (Figs. 2a, 3a, 4a, and 5a). The northern and southern parts of Chile have fewer high-mobility comunas. The comunas with the highest mobility registered during the pre-quarantine period are located in the regions of Metropolitana de Santiago, Arica y Parinacota, Valparaíso, Ñuble, and Magallanes (Table 3).

The top-ten comunas with the highest mobility indices change during the quarantine period, except for Rinconada in the region of Valparaíso (Table 4), mirroring the different degree of reduction in human mobility

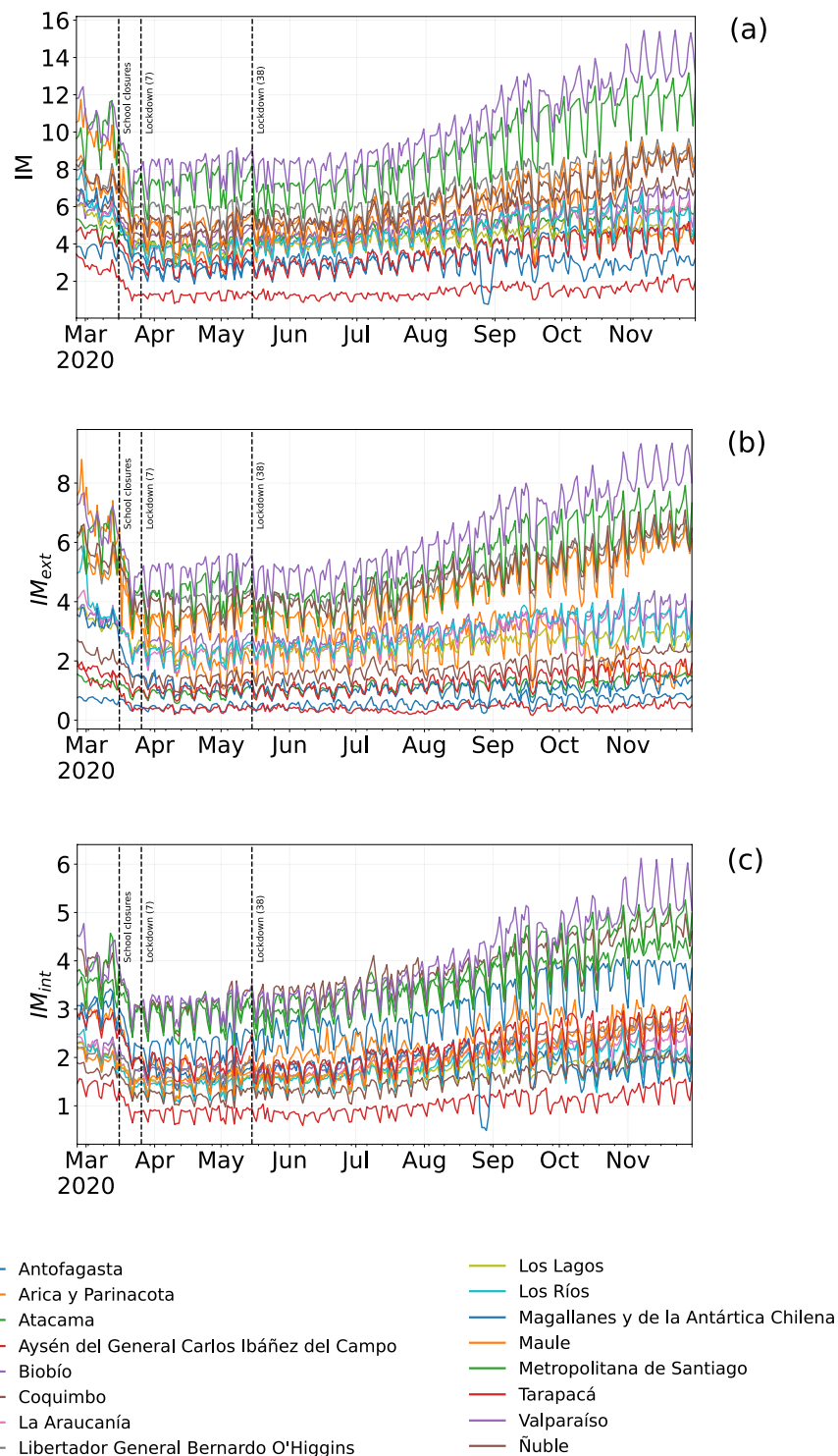


Fig. 7 Evolution of IM (a), IM_{ext} (b) and IM_{int} (c) from March to September 2020 for the 16 regions in Chile. The curves are sorted in descending order respect to the relative index of mobility of the corresponding comuna. The vertical lines denote important dates regarding NPIs in Chile; the number in parentheses indicates the number of comunas subject to that restriction.

in the Chilean regions (Fig. 6). All regions show a reduction in all three mobility indices during the quarantine period, albeit with different intensities (Fig. 7). At the comuna level, high-mobility comunas are rare and clustered near the large urban areas located in central Chile (Figs. 2–5).

These results are supported by the distributions of the mobility indices of the two periods (Fig. 8). There is a clear shift towards the left of the distribution of the IM index (Fig. 8a): (i) the average IM during the quarantine period (5.16 ± 2.74) is 27.6% lower than the average IM during the pre-quarantine period (7.13 ± 4.15); (ii) the

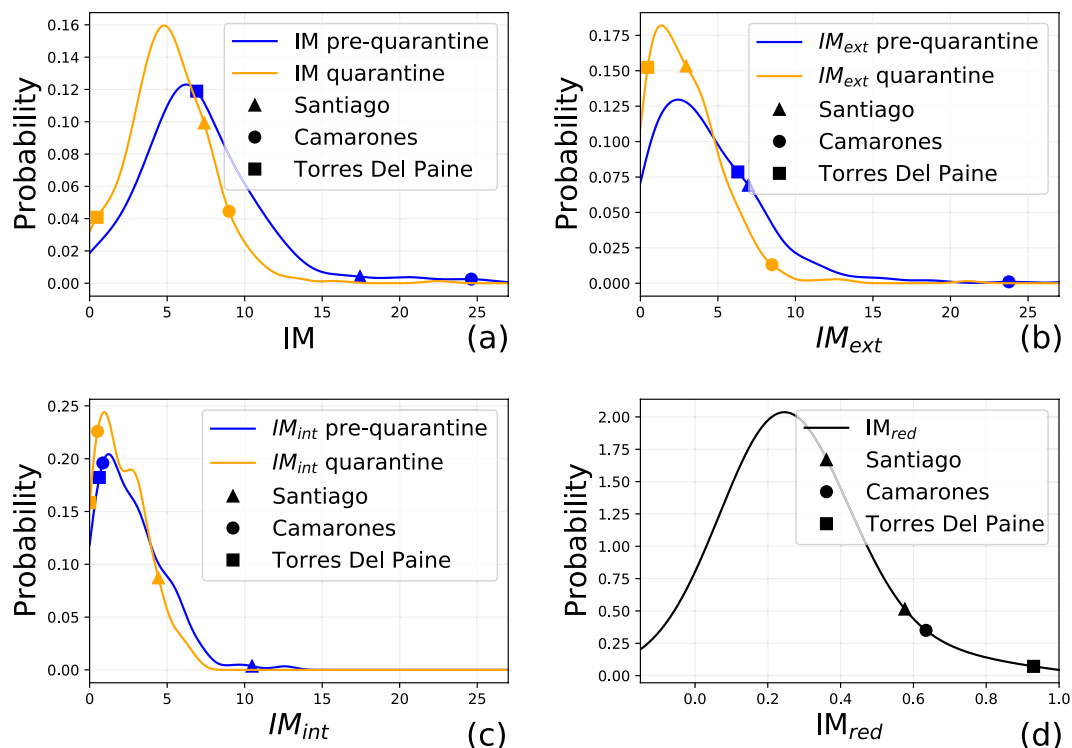


Fig. 8 Distributions of IM (a), IM_{ext} (b) and IM_{int} (c) for the pre-quarantine (blue) and quarantine (orange) periods, with the average values of three comunas: Santiago, Camarones and Torres Del Paine. (d) Distribution of IM_{red} for all the Chilean comunas.

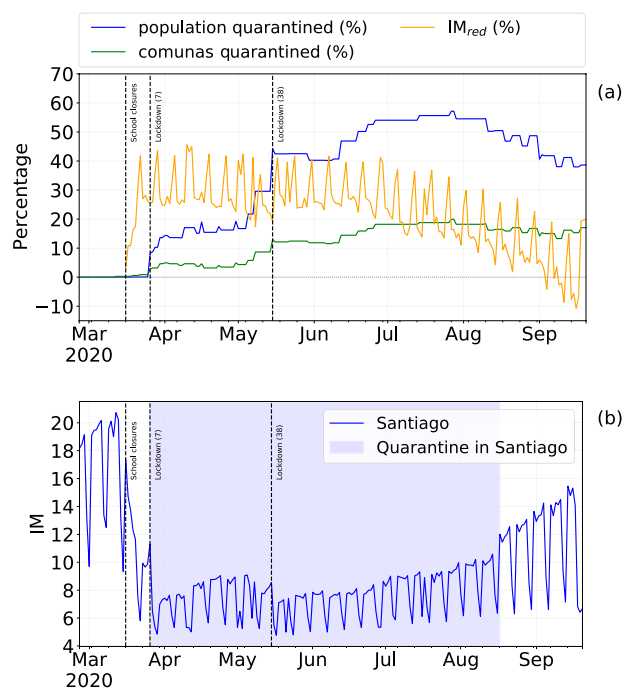


Fig. 9 (a) Percentage of population under quarantine and the percentage of mobility reduction IM_{red} from February 26th to September 20th, 2020. (b) Evolution of IM index in Santiago; the blue area denotes the quarantine period. The vertical lines denote important dates regarding NPIs in Chile; the number in parentheses indicates the number of comunas subject to that restriction.

distribution of IM during the quarantine period is more skewed to the left, showing a decrease of the mobility in Chile during the selected days. Regarding IM_{int} and IM_{ext} , we observe no net shift of the curve, but rather a flattening, suggesting that intra- and inter-comuna movements decreased during the quarantine (Fig. 8b,c).

We further analyze the reduction of the mobility defining IM_{red} as the relative reduction of the IM index in the quarantine period with respect to the pre-quarantine period. The distribution of IM_{red} shows that a large number of comunas have a reduced mobility, following Chilean government interventions, by an average of $25.37\% \pm 43.2$ (Fig. 8d). However, comunas that were not in quarantine during the quarantine period do not reduce their mobility significantly (Fig. 9a).

The percentage of population that live in comunas where the authorities applied NPIs increases with time (Fig. 9a) reaches its peak ($\approx 57\%$) in late July 2020. With the increase of the number of people under quarantine, IM_{red} initially increases, but it slightly decreases over time even if both the number of individuals and the number of comunas under quarantine increase. This phenomenon suggests that mobility restrictions are more effective in the short-medium term and become less effective as time goes by, and it can be observed both at regional (Fig. 7) and comuna level (Fig. 9a,b).

Unfortunately, we do not have ground truth data to compare our data with because there are no official indices at the comuna level in Chile. However, other mobility reports do exist for the same area and period at the regional level (not comunas), such as Google Mobility Reports¹³. By aggregating our data at the regional level and comparing them with Google's data, we find a strong Pearson correlation ($r = 0.7$), suggesting that our mobility index is reflecting mobility trends captured by other reliable data sources.

Limitations of our dataset. Mobile phone records are sparse and irregular in time, leading to gaps between the user's actual trajectory and the trajectory that can be inferred from their digital trace¹⁵. Chen *et al.*⁶⁰ propose an algorithm to reconstruct individual trajectories from CDRs by recovering the unspecified positions of each user. They revisit the seminal work of Gonzalez *et al.*²³, in which the authors show that heavy-tails characterise the distributions of (characteristic) distances traveled by individuals, showing that CDRs preserve the mobility patterns observed in the reconstructed (denser) trajectories, though slightly underestimating long trips and overestimating short ones⁶⁰. Considering that in our study we use XDRs, which are way denser than CDRs, we can assume that the mobility traces of individuals represented in our dataset do not differ significantly from the actual user's trajectory.

Code availability

The up-to-date data are available from the general repository of the Ministry of Science of Chile at: <https://raw.githubusercontent.com/MinCiencia/Datos-COVID19/master/output/producto33/IndiceDeMovilidad.csv> (IM indices), and <https://github.com/MinCiencia/Datos-COVID19/blob/master/output/producto29/Cuarentenas-Activas.csv> (quarantines). The code to download the up-to-date data automatically and to reproduce the analysis in our paper is available at⁵⁸.

Received: 9 December 2020; Accepted: 8 December 2022;

Published online: 03 January 2023

References

- Dong, E., Du, H. & Gardner, L. An interactive web-based dashboard to track covid-19 in real time. *The Lancet infectious diseases* **20**, 533–534 (2020).
- Lai, S. *et al.* Effect of non-pharmaceutical interventions to contain COVID-19 in china. *Nature* **585**, 410–413 (2020).
- Haushofer, J. & Metcalf, C. J. E. Which interventions work best in a pandemic? *Science* **368**, 1063–1065 (2020).
- Gao, S., Rao, J., Kang, Y., Liang, Y. & Kruse, J. Mapping county-level mobility pattern changes in the united states in response to covid-19. *SIGSpatial Special* **12**, 16–26 (2020).
- Chinazzi, M. *et al.* The effect of travel restrictions on the spread of the 2019 novel coronavirus (covid-19) outbreak. *Science* **368**, 395–400 (2020).
- Gatto, M. *et al.* Spread and dynamics of the covid-19 epidemic in italy: Effects of emergency containment measures. *Proceedings of the National Academy of Sciences* **117**, 10484–10491 (2020).
- Jia, J. S. *et al.* Population flow drives spatio-temporal distribution of covid-19 in china. *Nature* 1–5 (2020).
- Tian, H. *et al.* An investigation of transmission control measures during the first 50 days of the covid-19 epidemic in china. *Science* **368**, 638–642 (2020).
- Lucchini, L. *et al.* Living in a pandemic: changes in mobility routines, social activity and adherence to COVID-19 protective measures. *Scientific Reports* **11**, 24452, <https://doi.org/10.1038/s41598-021-04139-1> (2021).
- Gozzi, N. *et al.* Estimating the effect of social inequalities on the mitigation of covid-19 across communities in santiago de chile. *Nature communications* **12**, 1–9 (2021).
- Ferres, L. *et al.* Measuring levels of activity in a changing city. Tech. Rep., Institute of Data Science, Universidad del Desarrollo. https://datascience.udd.cl/covid_ids_tef_01.pdf (2020).
- Buckee, C. O. *et al.* Aggregated mobility data could help fight covid-19. *Science (New York, NY)* **368**, 145 (2020).
- Aktay, A. *et al.* Google covid-19 community mobility reports: Anonymization process description (version 1.1). <https://arxiv.org/abs/2004.04145> (2020).
- Luca, M., Barlacchi, G., Lepri, B. & Pappalardo, L. A survey on deep learning for human mobility. *ACM Comput. Surv.* **55**. <https://doi.org/10.1145/3485125> (2021).
- Blondel, V. D., Decuyper, A. & Krings, G. A survey of results on mobile phone datasets analysis. *EPJ Data Science* **4**, 10 (2015).
- Barbosa, H. *et al.* Human mobility: Models and applications. *Physics Reports* **734**, 1–74 (2018).
- Andrienko, G. *et al.* (so) big data and the transformation of the city. *International Journal of Data Science and Analytics* **11**, 311–340 (2021).
- Pappalardo, L., Simini, F., Barlacchi, G. & Pellungrini, R. scikit-mobility: A Python Library for the Analysis, Generation, and Risk Assessment of Mobility Data. *Journal of Statistical Software* **103**, 1–38, <https://www.jstatsoft.org/index.php/jss/article/view/v103i04> (2022).
- Gabrielli, L., Furetti, B., Trasarti, R., Giannotti, F. & Pedreschi, D. City users' classification with mobile phone data. *2015 IEEE International Conference on Big Data (Big Data)* 1007–1012 (2015).

20. Deville, P. *et al.* Dynamic population mapping using mobile phone data. *Proceedings of the National Academy of Sciences* **111**, 15888–15893 (2014).
21. Pappalardo, L., Ferres, L., Sacasa, M., Cattuto, C. & Bravo, L. Evaluation of home detection algorithms on mobile phone data using individual-level ground truth. *EPJ Data Science* **10**, 29, <https://doi.org/10.1140/epjds/s13688-021-00284-9> (2021).
22. Alessandretti, L., Sapiezynski, P., Sekara, V., Lehmann, S. & Baronchelli, A. Evidence for a conserved quantity in human mobility. *Nature Human Behaviour* **2**, 485–491 (2018).
23. Gonzalez, M. C., Hidalgo, C. A. & Barabási, A.-L. Understanding individual human mobility patterns. *nature* **453**, 779–782 (2008).
24. Pappalardo, L. *et al.* Returners and explorers dichotomy in human mobility. *Nature Communications* **6** (2015).
25. Song, C., Qu, Z., Blumm, N. & Barabási, A.-L. Limits of predictability in human mobility. *Science* 1018–1021 (2010).
26. Pappalardo, L. & Simini, F. Data-driven generation of spatio-temporal routines in human mobility. *Data Mining and Knowledge Discovery* **32**, 787–829 (2018).
27. Hankaew, S. *et al.* Inferring and modeling migration flows using mobile phone network data. *IEEE Access* **7**, 164746–164758 (2019).
28. Balzotti, C., Bragagnini, A., Briani, M. & Cristiani, E. Understanding human mobility flows from aggregated mobile phone data. *IFAC-PapersOnLine* **51**, 25–30 (2018).
29. Bonnel, P., Fekih, M. & Smoreda, Z. Origin-destination estimation using mobile network probe data. *Transportation Research Procedia* **32**, 69–81 (2018).
30. Simini, F., Barlacchi, G., Luca, M. & Pappalardo, L. A Deep Gravity model for mobility flows generation. *Nature Communications* **12**, 6576, <https://doi.org/10.1038/s41467-021-26752-4> (2021).
31. Pappalardo, L. *et al.* An analytical framework to nowcast well-being using mobile phone data. *International Journal of Data Science and Analytics* **2**, 75–92 (2016).
32. Eagle, N., Macy, M. & Claxton, R. Network diversity and economic development. *Science* **328**, 1029–1031 (2010).
33. Frias-Martinez, V., Virseda-Jerez, J. & Frias-Martinez, E. On the relation between socio-economic status and physical mobility. *Information Technology for Development* **18**, 91–106 (2012).
34. Šćepanović, S., Mishkovski, I., Hui, P., Nurminen, J. K. & Ylä-Jääski, A. Mobile phone call data as a regional socio-economic proxy indicator. *PLoS ONE* **10**, e0124160 (2015).
35. Mao, H., Shuai, X., Ahn, Y.-Y. & Bollen, J. Quantifying socio-economic indicators in developing countries from mobile phone communication data: applications to côte d’ivoire. *EPJ Data Science* **4**, 15 (2015).
36. Voukelatou, V. *et al.* Measuring objective and subjective well-being: dimensions and data sources. *International Journal of Data Science and Analytics* **11**, 279–309 (2021).
37. de Montjoye, Y.-A. *et al.* On the privacy-conscious use of mobile phone data. *Nature Scientific Data* **5**, 180286 (2018).
38. de Montjoye, Y.-A., Hidalgo, C. A., Verleysen, M. & Blondel, V. D. Unique in the crowd: The privacy bounds of human mobility. *Scientific Reports* **3** (2013).
39. Pellungrini, R., Pappalardo, L., Pratesi, F. & Monreale, A. A data mining approach to assess privacy risk in human mobility data. *ACM Transactions on Intelligent Systems and Technologies* **9**, 31:1–31:27 (2017).
40. Fiore, M. *et al.* Privacy in trajectory micro-data publishing: a survey. *Transactions on Data Privacy* **13**, 91–149 (2020).
41. Oliver, N. *et al.* Mobile phone data for informing public health actions across the covid-19 pandemic life cycle. *Science Advances* **6** (2020).
42. Finger, F. *et al.* Mobile phone data highlights the role of mass gatherings in the spreading of cholera outbreaks. *Proceedings of the National Academy of Sciences* **113**, 6421–6426 (2016).
43. Tizzoni, M. *et al.* On the use of human mobility proxies for modeling epidemics. *PLoS Comput Biol* **10**, e1003716 (2014).
44. Wesolowski, A. *et al.* Quantifying the impact of human mobility on malaria. *Science* **338**, 267–270 (2012).
45. Bengtsson, L. *et al.* Using mobile phone data to predict the spatial spread of cholera. *Scientific reports* **5**, 8923 (2015).
46. Kang, Y. *et al.* Multiscale dynamic human mobility flow dataset in the us during the covid-19 epidemic. *Scientific Data* **7**, 1–13 (2020).
47. Kraemer, M. U. G. *et al.* The effect of human mobility and control measures on the covid-19 epidemic in china. *Science* **368**, 493–497 (2020).
48. Pullano, G., Valdano, E., Scarpa, N., Rubrichi, S. & Colizza, V. Evaluating the effect of demographic factors, socioeconomic factors, and risk aversion on mobility during the covid-19 epidemic in france under lockdown: a population-based study. *The Lancet Digital Health* **2**, e638–e649 (2020).
49. Badr, H. S. *et al.* Association between mobility patterns and covid-19 transmission in the usa: a mathematical modelling study. *The Lancet Infectious Diseases* **20**, 1247–1254 (2020).
50. Bakker, M., Berke, A., Groh, M., Pentland, A. & Moro, E. Effect of social distancing measures in the new york city metropolitan area. Tech. Rep., Massachusetts Institute of Technology (2020).
51. Han, S. Y., Tsou, M.-H., Knaap, E., Rey, S. & Cao, G. How do cities flow in an emergency? tracing human mobility patterns during a natural disaster with big data and geospatial data science. *Urban Science* **3**, 51 (2019).
52. Xu, Y. & González, M. C. Collective benefits in traffic during mega events via the use of information technologies. *Journal of The Royal Society Interface* **14**, 20161041 (2017).
53. Zhang, J., Zheng, Y. & Qi, D. Deep spatio-temporal residual networks for citywide crowd flows prediction. In *Thirty-First AAAI Conference on Artificial Intelligence* (2017).
54. Xie, P. *et al.* Urban flow prediction from spatiotemporal data using machine learning: A survey. *Information Fusion* **59**, 1–12 (2020).
55. Yin, X. *et al.* A Comprehensive Survey on Traffic Prediction. Preprint at <https://arxiv.org/abs/2004.08555> (2020).
56. Vanhoof, M., Reis, F., Ploetz, T. & Smoreda, Z. Assessing the quality of home detection from mobile phone data for official statistics. *Journal of Official Statistics* **34**, 935–960 (2018).
57. Telefónica Chile. Condiciones contractuales del servicio telefónico móvil <https://www2.movistar.cl/terminos-regulaciones/condiciones-comerciales-y-contractuales-movil/pdf/CondicionesContractualesTelefonicoMovil.pdf> (2020).
58. Ferres, L., Pappalardo, L., Cornacchia, G., Bravo, L. & Navarro-Aranguez, V. Mobility index for local quarantines in chile. *figshare* <https://doi.org/10.6084/m9.figshare.c.5214272.v7> (2021).
59. Instituto Nacional de Estadísticas de Chile. Censo 2017 comuna: Población, viviendas por área y densidad <https://geoine-ine-chile.opendata.arcgis.com/search?tags=Capas%20Base> (2020).
60. Chen, G., Viana, A., Fiore, M. & Sarraute, C. Complete trajectory reconstruction from sparse mobile phone data. *EPJ Data Science* **8** (2019).

Acknowledgements

Luca Pappalardo and Giuliano Cornacchia have been funded by 1) EU project SoBigData++ RI grant #871042, and 2) NextGenerationEU - National Recovery and Resilience Plan (Piano Nazionale di Ripresa e Resilienza, PNRR), project “SoBigData.it - Strengthening the Italian RI for Social Mining and Big Data Analytics”, prot. IR0000013, avviso n. 3264 on 28/12/2021. Leo Ferres and Loreto Bravo thank the funding and support of Telefónica R&D Chile and CISCO Chile. This research was supported by FONDECYT Grant N°1130902 to Loreto Bravo and FONDECYT Grant N°1221315 to Leo Ferres. We thank Daniele Fadda for his support on data visualization.

Author contributions

L.F., V.N. and L.B. developed and computed the mobility indices. L.P., L.F. and G.C. analyzed the data, made the plots and wrote the paper.

Competing interests

The authors declare no competing interests.

Additional information

Correspondence and requests for materials should be addressed to L.F.

Reprints and permissions information is available at www.nature.com/reprints.

Publisher's note Springer Nature remains neutral with regard to jurisdictional claims in published maps and institutional affiliations.



Open Access This article is licensed under a Creative Commons Attribution 4.0 International License, which permits use, sharing, adaptation, distribution and reproduction in any medium or format, as long as you give appropriate credit to the original author(s) and the source, provide a link to the Creative Commons license, and indicate if changes were made. The images or other third party material in this article are included in the article's Creative Commons license, unless indicated otherwise in a credit line to the material. If material is not included in the article's Creative Commons license and your intended use is not permitted by statutory regulation or exceeds the permitted use, you will need to obtain permission directly from the copyright holder. To view a copy of this license, visit <http://creativecommons.org/licenses/by/4.0/>.

© The Author(s) 2023